Jordan Journal of Civil Engineering, Volume **12**, No. **1**, **2018**

The Effect of Beam Design on Behaviour of Retrofitted Beam Using CFRP

Yasmeen Taleb Obaidat

Department of Civil Engineering, Jordan University of Science and Technology (JUST), Irbid, Jordan.
E-Mail: ytobeidat@just.edu.jo

ABSTRACT

Debonding is the prevailing failure mode in the retrofitted RC beam using carbon fibre-reinforced polymer (CFRP). Therefore, this issue should be given more concern. A non-linear 3D numerical model was used to study the effects of different parameters on the failure mechanisms and load capacity of retrofitted beam by CFRP. These parameters were: internal tensile reinforcement, internal shear reinforcement, pre-crack number and beam width. In addition, this paper deals with the effect of mesh sensitivity on modelling retrofitted beam behaviour. The non-linear behaviours of concrete, steel and the interface between concrete and CFRP were taken into consideration. It was found that mesh sensitivity plays a role in representing the behaviour of retrofitted beam with CFRP. The results indicate that internal tensile reinforcement, internal shear reinforcement, pre-crack number and beam width have significant effects on the percentage of load increase and strain in CFRP.

KEYWORDS: Carbon fibre-reinforced plastic (CFRP), Strengthening, Laminate, Isotropic, Cohesive model, Reinforced concrete beam.

INTRODUCTION

In recent years, the application of fibre-reinforced polymer (FRP) as external reinforcement has received much attention. However, there is a problem of possible premature failure due to debonding of the FRP plates when these materials are used for retrofitting reinforced concrete RC structures.

Debonding is a critical problem associated with retrofitted structures using FRP and prevents full utilization of FRP. Information on the effectiveness of several parameters is still not completely understood. Therefore, parameters that affect debonding should be given more concern. To help overcome this drawback, this study looks into several parameters that affect FRP-strengthened structure elements using finite element model (FEM).

Non-linear FE analysis can be used to study the behaviour of retrofitted beams. Recently, researchers have attempted to simulate the behaviour of RC beams retrofitted by FRP using finite element techniques. The complex behaviour of retrofitted RC structures led researchers to use a linear elastic analysis to address the interfacial behaviour before cracking. A more advanced finite element model was introduced to take into consideration the material non-linearities of concrete (Pannirselvam et al., 2008; Supaviriyakit et al., 2004; Yang et al., 2003). These analytical models were proposed to predict the load-deflection behaviour and the ultimate load carrying capacity of FRP- retrofitted RC beams, but not to simulate the debonding failure modes or address the interfacial behaviour through the interface. To accurately predict the ultimate load carrying capacity and the debonding failure of FRP-retrofitted RC beams, it is necessary to model the bond

Received on 22/6/2017.
Accepted for Publication on 4/10/2017.

at the FRP/concrete interface. The interface elements must be able to capture the interfacial non-linearities and contain an appropriate failure criterion to predict the debonding failure. This has already been done by Obaidat et al. (2010).

The work presented in this paper utilizes the finite element method to characterize the effects of internal tensile reinforcement, internal shear reinforcement, pre-crack number and beam width on the overall behaviour of carbon fibre-reinforced polymer (CFRP)-retrofitted beams.

Finite Element Model

The plastic damage model was used for modelling the non-linear behaviour of concrete. The model assumes that the two main failure mechanisms are tensile cracking and compressive crushing. The concrete behaviour in tension was modelled using linear elastic approach until cracking is initiated at tensile strength. Beyond crack initiation, the formation of micro-cracks is represented with a softening response. The softening curve of concrete under tension was represented using Hillerborg (1985), see Figure 1.

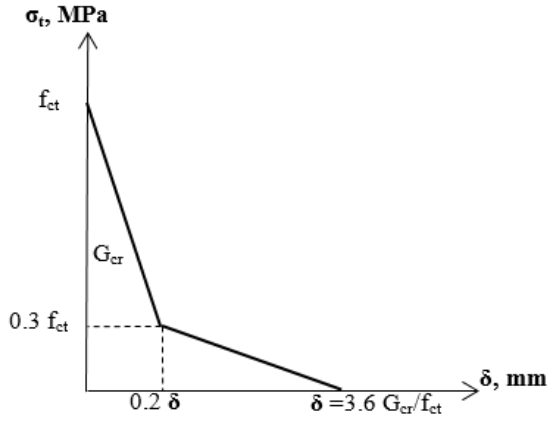

Figure (1): Post-peak stress deformation relationship for concrete under uni-axial tension

The initial Young's modulus of concrete (E_c) is reasonably calculated using Eq. (1) given by ACI 318M-08 (2008):

$$E_c = 4700\sqrt{f'_c} \quad (1)$$

Values for fracture energy G_{cr} (Nmm/mm^2) can be obtained by using Eq. (2) (CEB-FIP, 1993):

$$G_{cr} = G_{fo} * (0.1 * f_c)^{0.7} \quad (2)$$

where:

f_c: concrete compressive strength (MPa).

G_{fo}: base value for fracture energy (N.mm/mm^2), which depends on maximum aggregate size as shown in Table 1.

Table 1. Base values for fracture energy (CEB-FIP, 1993)

Maximum aggregate size d_{max} (mm)	Fracture energy G_{fo} (N.mm/mm^2)
8	0.025
16	0.030
32	0.058

Concrete stress-strain behaviour in compression was described using a suitable model developed by Saenz (1964):

$$\sigma_c = \frac{E_c \varepsilon_c}{1+(R+R_E-2)\left(\frac{\varepsilon_c}{\varepsilon_0}\right)-(2R-1)\left(\frac{\varepsilon_c}{\varepsilon_0}\right)^2+R\left(\frac{\varepsilon_c}{\varepsilon_0}\right)^3} \quad (3)$$

where:

$$R = \frac{R_E(R_\sigma-1)}{(R_\varepsilon-1)^2} - \frac{1}{R_\varepsilon}, \quad R_E = \frac{E_c}{E_0}$$

$$E_0 = \frac{f'_c}{\varepsilon_0} \quad (4)$$

and ε_0 = 0.0025, $R_\varepsilon = 4$, $R_\sigma = 4$, as reported in Hu and Schnobrich (1989).

Poisson's ratio for concrete was assumed to be 0.2.

The steel reinforcement is simplified in the model by ignoring the horizontal portions of the stirrup steel present in the test beams. Ideally, the bond strength between the concrete and steel reinforcement should be considered. However, in this study, perfect bond

between materials is assumed. The steel was assumed to be an elastic-perfectly plastic material. The CFRP material was assumed to be isotropic with linear elasticity until failure.

The interface response between concrete and CFRP was modelled using cohesive element (bilinear traction separation). The parameters in this model are: initial stiffness, K_0, shear strength, τ_{max} and fracture energy, G_f. Those were determined according to Obaidat et al. (2013):

$$K_0 = 0.16(G_a/t_a) + 0.47 \quad (5)$$

$$\tau_{max} = 1.46 \times ((G_a)^{0.165} \times (f_{ct})^{1.033}) \quad (6)$$

$$G_f = 0.52 \times (f_{ct})^{0.26} \times (G_a)^{-0.23} \quad (7)$$

where t_a is the adhesive layer thickness, G_a is the shear modulus of the adhesive and f_{ct} is the tensile strength of concrete in MPa.

This paper is a continuation of another paper by Obaidat et al. (2010). Herein, we investigate the variance meshes and prametric study by using the method developed in that paper (Obaidat et al., 2010). The numerical calculations are performed for four beams studied by Obaidat et al. (2011) that were used to validate the finite element model in this paper. The beams were identical in geometry and tested with four-point loadings, see Figure 2. Two beams were tested as control beams, while the other two were loaded until cracks appeared, then retrofitted with unidirectional CFRP at the bottom of the beams between two supports and retested to failure. The elastic modulus, E_s, and yield stress, f_y, were measured in the experimental study and the values obtained were E_s= 209 GPa and f_y= 507 MPa. The elastic modulus was taken as 165 GPa as in the experimental work. The Poisson's ratio of CFRP was assumed to be ν = 0.3.

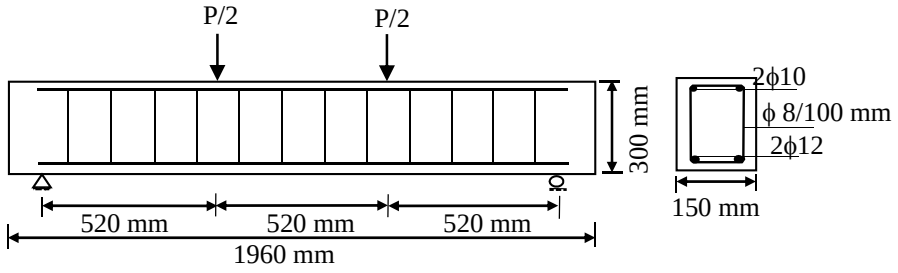

Figure (2): Geometry, arrangement of reinforcement and load of the tested beams

By taking advantage of the symmetry of the beams, a quarter of the full beam is used for modelling with proper boundary conditions. The FE analyses were performed under displacement control. The boundary conditions for the simulated quarter of beam are illustrated in Figure 3. Load was applied in a location corresponding to experimental work.

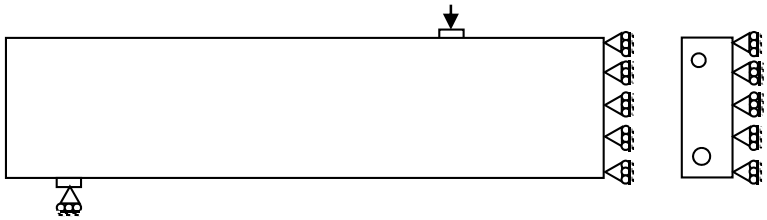

Figure (3): Boundary conditions used in numerical work

4-node linear tetrahedral elements were used for concrete, reinforcement steel, steel plates at supports and under the load and CFRP. 3-D 8-node cohesive elements were used to model the interface layer. Small enough time increments were used to ensure that the analysis will follow the load-deflection curve and this improved convergence. Tied contact was used for connection meshes between concrete and cohesive element, between cohesive element and CFRP and between steel plate and concrete.

Validation and Mesh Sensitivity

As previously mentioned, this work is a continuation of a paper by Obaidat et al. (2010). This study shows the effect of element size. Three meshes were used for studying mesh sensitivity, see Figure 4.

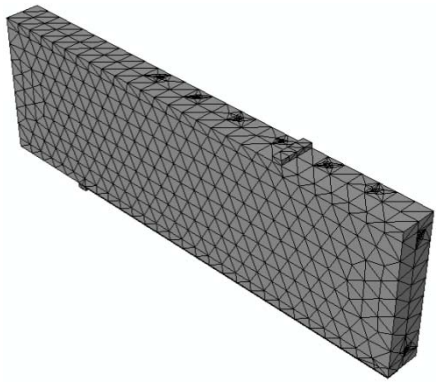

(a) Coarse mesh, 100505 linear tetrahedral elements, 39 cohesive elements

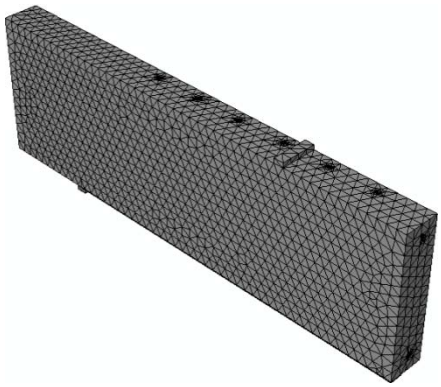

(b) Fine mesh, 168630 linear tetrahedral elements, 39 cohesive elements

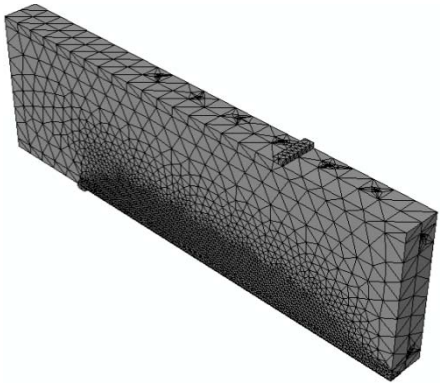

(c) A fine mesh at constant moment region, 169623 linear tetrahedral elements, 39 cohesive elements

Figure (4): Finite element mesh of quarter of beam

This shows that all models can reflect the real behaviour with accuracy, which may be acceptable for engineering solutions. The study also shows that larger elements give lower stiffness and small elements reflect better individual cracks, due to better strain localization. Higher response was also reached by larger number of elements around the constant moment region, see Figure 5.

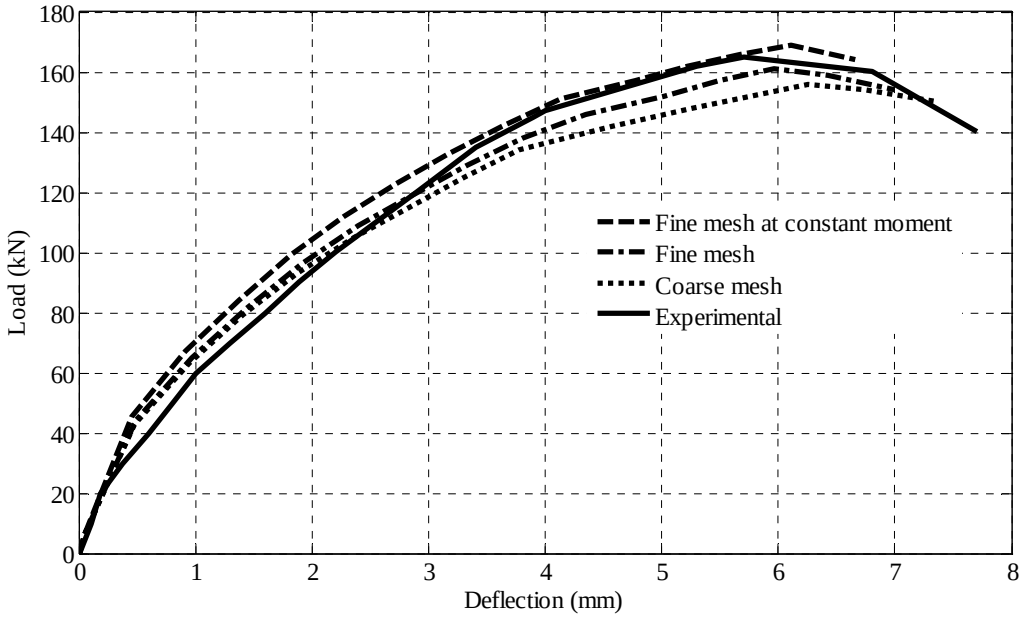

Figure (5): Load *versus* mid-span deflection for mesh cases and experimental work

It is clear from Figure 6 that if the number of elements around the constant moment region increases, the element size is equal to or smaller than the crack spacing, the crack pattern would be close to the experimental crack. This means that results obtained from a fine mesh around constant moment were more accurate. Therefore, this mesh was chosen to complete the remaining part of this study.

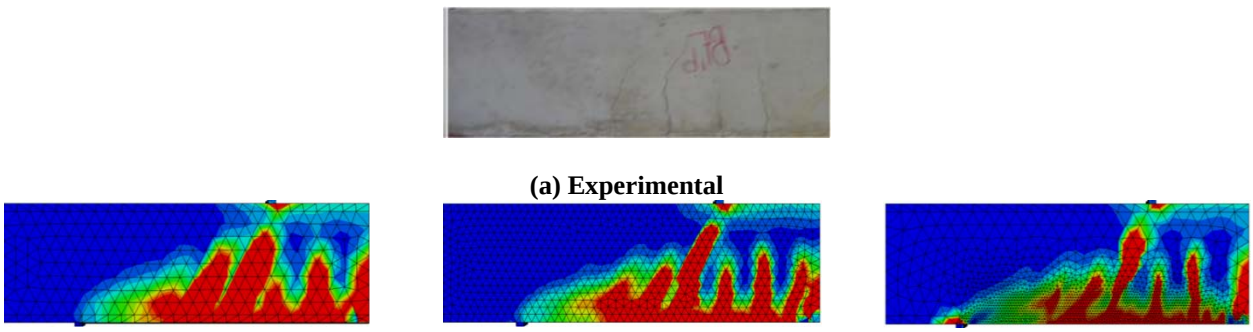

(a) Experimental

(b) Coarse mesh **(c) Fine mesh** **(d) A fine mesh at constant moment region**

Figure (6): Crack pattern of retrofitted beam obtained from experimental and numerical works

Parametric Study

Even though there have been a large number of experimental studies, the failure mechanisms are still not fully understood and the influences of several parameters are not yet proved. Many parameters play roles in the behaviour of retrofitted beam. In this study, several parameters were taken into consideration. These are: internal longitudinal steel, internal shear steel, pre-crack

number and beam width. The results for each parameter are shown separately in the following sub-sections.

Reinforcement Steel

By fixing the other parameters, the diameter of internal tension reinforcement was studied by varying it as follows: 16 mm, 14 mm, 12 mm and 10 mm. This represents the deterioration of steel in reality. When corrosion occurs, the steel will lose a part of its cross-section.

The effect of internal tension reinforcement was evaluated based on its response to percentage of increasing load and CFRP strain distribution *versus* distance from mid-span.

As shown in Figure 7, the higher diameter model provides a higher load than the lower diameter models. This may be attributed to the higher diameter model being capable of delaying the initiation of micro-cracks.

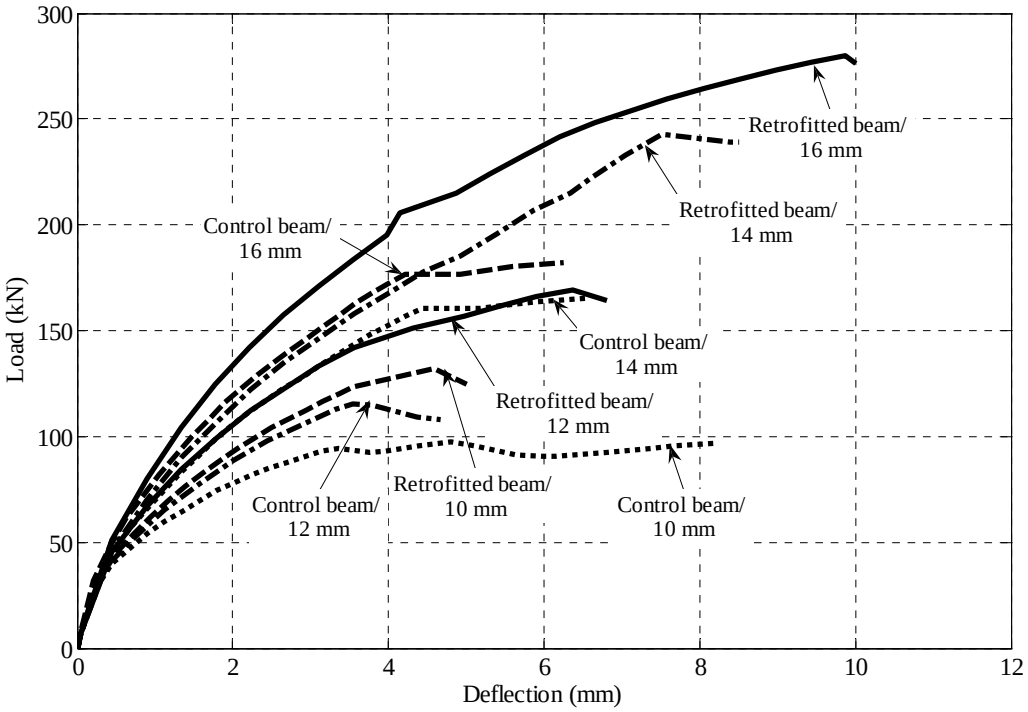

Figure (7): Load *versus* mid-span deflection for internal tensile reinforcement models

Figure 8 shows the percentage of increasing load for each diameter. The figure clearly demonstrates that when the diameter of internal steel increases, the percentage of increasing load increases. A possible explanation to why the lower diameter model has small enhancement of load capacity as compared to the higher diameter model may be attributed to the initiation of macro-crack debonding that occurs after steel yielding at lower load for low ratio of reinforcement compared to high ratio of reinforcement.

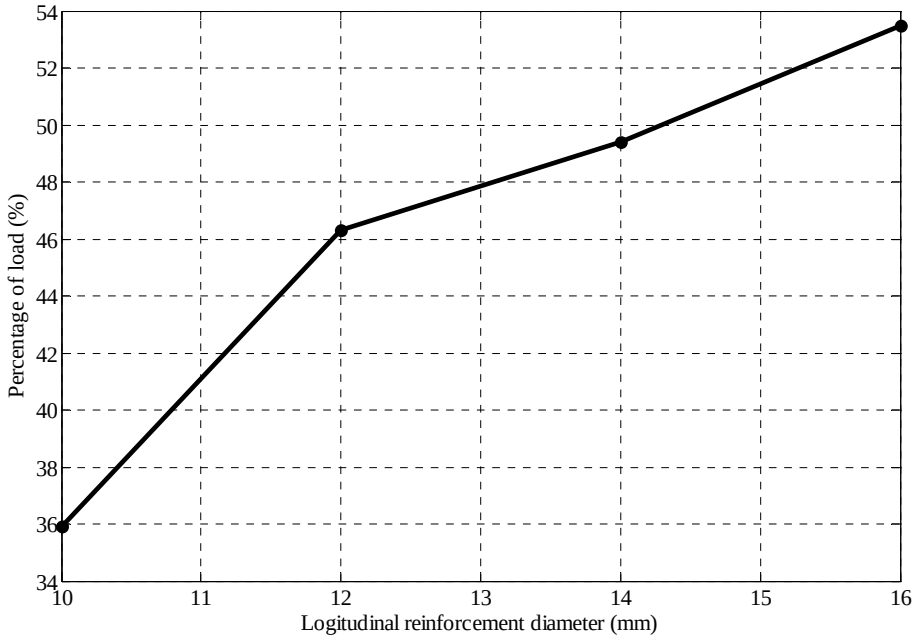

Figure (8): The percentage of increasing load capacity for tensile reinforcement cases

Figure 9 illustrates the strain in the CFRP plate. The increase in the CFRP strain when the reinforcement diameter decreases can be attributed to the fact that the CFRP is required to restrain the opening of the flexural crack, since the steel has yielded earlier while loading continued to increase. Complete debonding was found to be as shown in Figure 10.

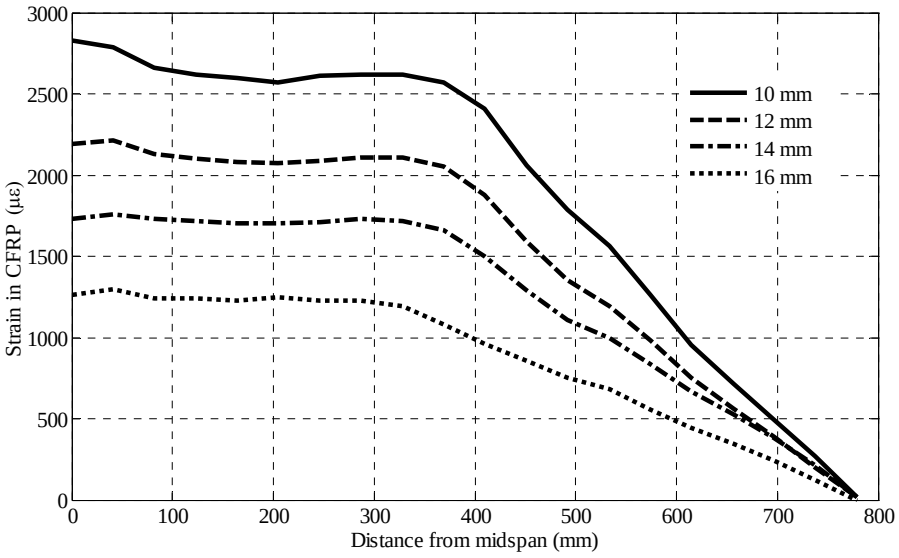

Figure (9): Axial strain in CFRP layer for reinforcement cases at steel yielding

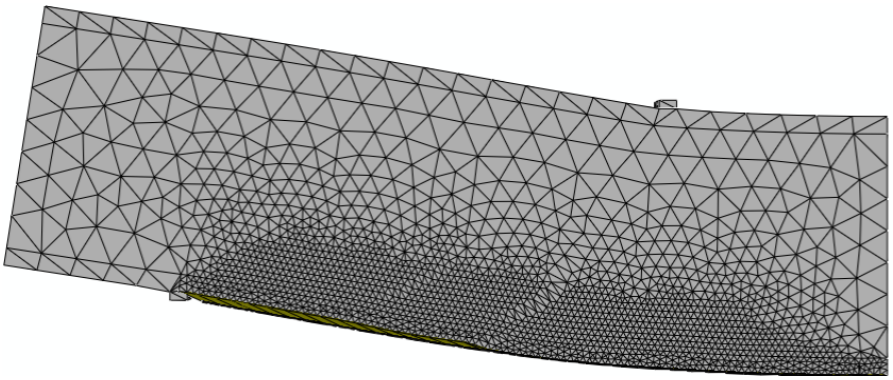

Figure (10): Failure modes for reinforcement cases

Internal Shear Steel

To study the effect of shear capacity on the beam retrofitted with CFRP, different shear capacities were used. This was represented by different spaces between the stirrups. The spaces were 50 mm, 100 mm, 200 mm and 400 mm.

From this study, the internal shear steel indicated a strong effect on the behaviour of the retrofitted beam. Figure 11 shows load *versus* mid-span deflection for parametric analysis. The figure clearly shows that the load increases with decreasing the space between the stirrups. This can be attributed to the fact that large space between stirrups yields creating earlier shear crack, causing the beam failure to occur earlier.

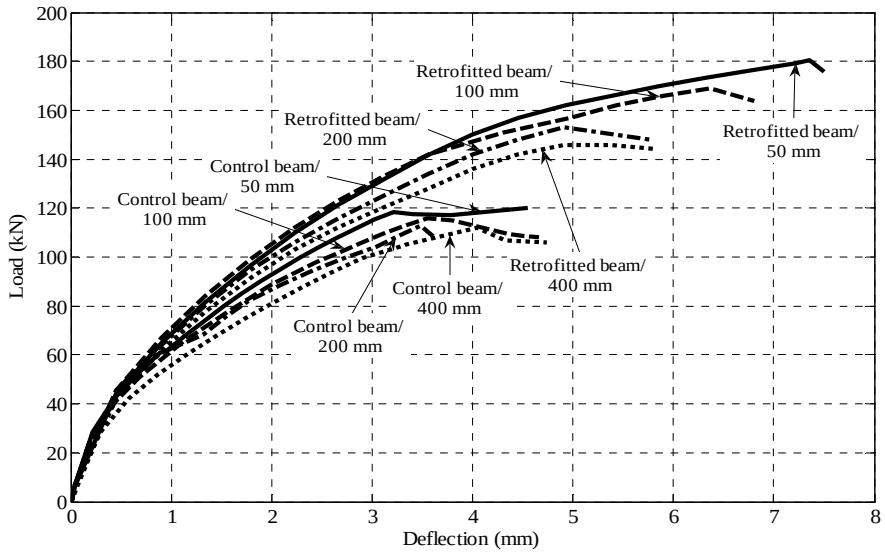

Figure (11): Load *versus* mid-span deflection for internal shear reinforcement models

From Figure 12, it can be seen that the percentage of load increases with the decrease in the space between the stirrups (increase in shear capacity). This can be explained by the fact that intensive stirrups restrict the formation of shear cracks; thus, the concentration of stress decreases, resulting in delaying debonding.

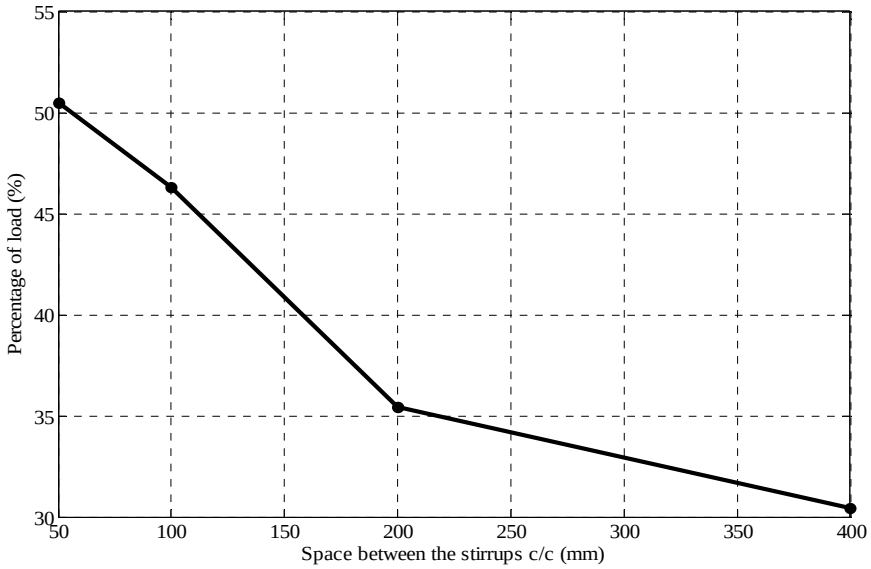

Figure (12): The percentage of increasing load capacity for shear capacity cases

Figure 13 illustrates the CFRP strain distribution for all cases. The figure exemplifies how lower shear capacity contributes to utilizing the retrofitting system, as the strain of the CFRP is noticeably greater when lower shear capacity was employed. This is attributed to that higher shear capacity delays the onset of macro-cracks, then decreases the transfer of load between concrete and CFRP.

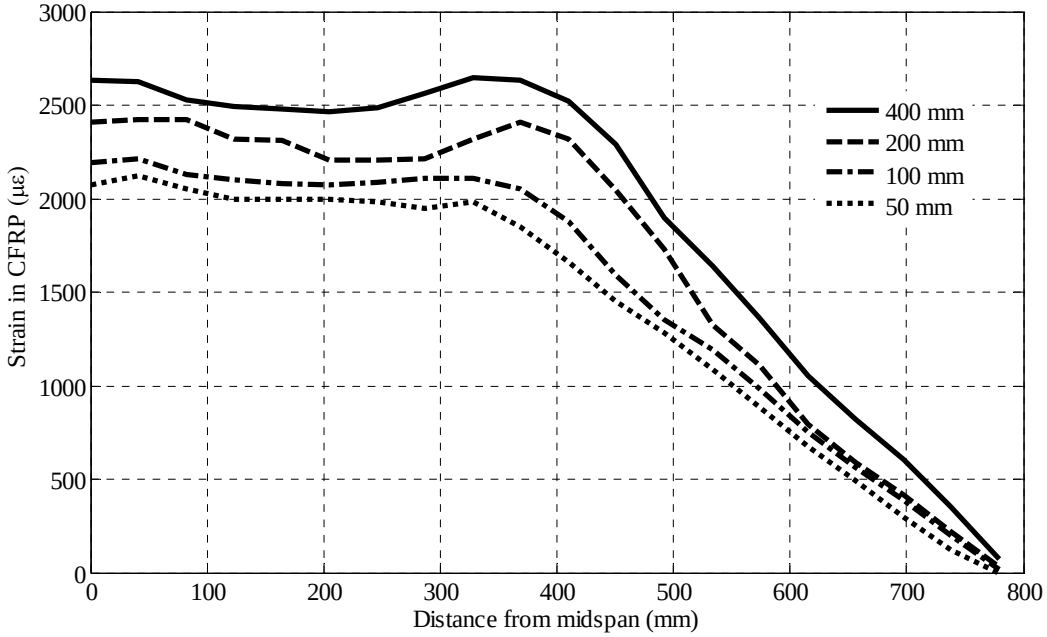

Figure (13): Axial strain in CFRP layer for shear capacity cases at steel yielding

It can be concluded from this study that if the shear capacity of the beam is sufficiently high, potential debonding failure is most likely to take place through CFRP debonding at the area of high stress concentration at laminate end and propagate to the mid-span of the beam as shown in Fig. 10. For lower shear capacity, the failure mode was debonding associated with shear cracking.

Pre-crack Number

To study the effect of crack number on the behaviour of the CFRP-concrete system, different numbers of flexural cracks were predefined in models 2, 4 and 6 spaced at 20 mm from the mid-span and 50 mm between each other.

The flexural crack number was found to significantly affect the structure stiffness, strain in CFRP and load carrying capacity of CFRP-concrete system. From Figure 14, it can be seen that structural stiffness, as well as maximum load increase as crack number decreases. From Figure 15, it can be seen that the crack number affects the strain in CFRP. It can be noticed from Figure 15 that strain for large crack number increases due to the fact that increasing the crack number increases stress transfer between CFRP and concrete. Large crack number causes the concrete to be easy to crack, since the concrete becomes weaker.

For all models, the failure mode was due to end plate debonding.

Beam Width

In this sub-section, a series of FE results for different beam widths are demonstrated. Three sets of beam widths are considered here, which are 100, 150 and 200 mm with keeping the ratio of internal reinforcement and external reinforcement constant. Figure 16 shows the load *versus* mid-span deflection for the parametric analysis. It can be seen that higher beam width model gives higher stiffness and load.

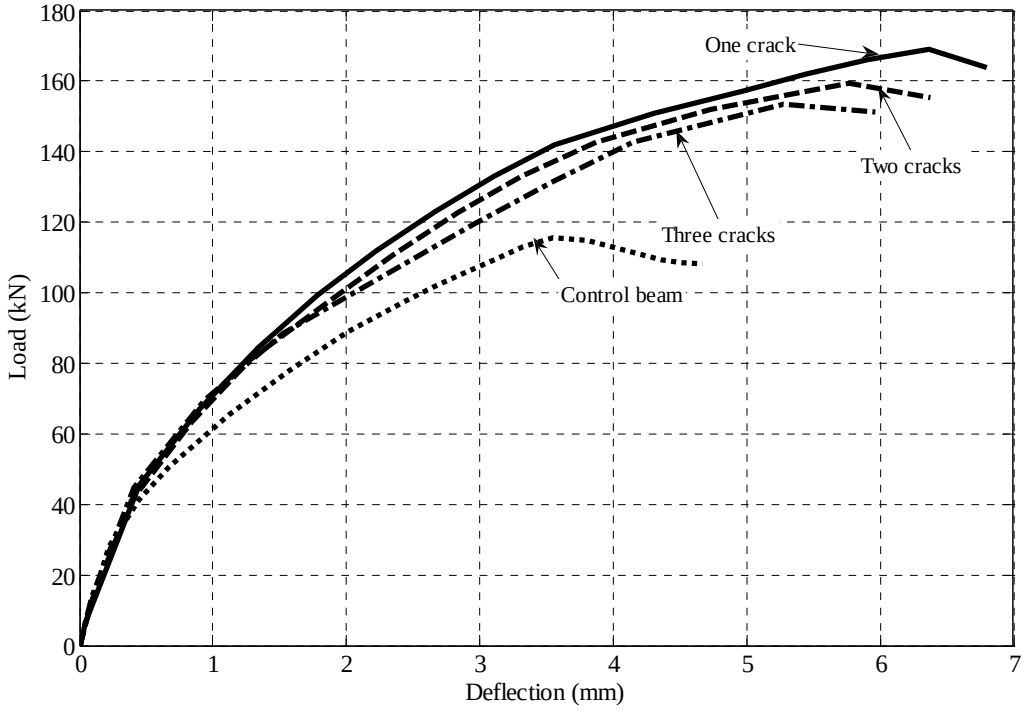

Figure (14): Load *versus* mid-span deflection for pre-crack width cases

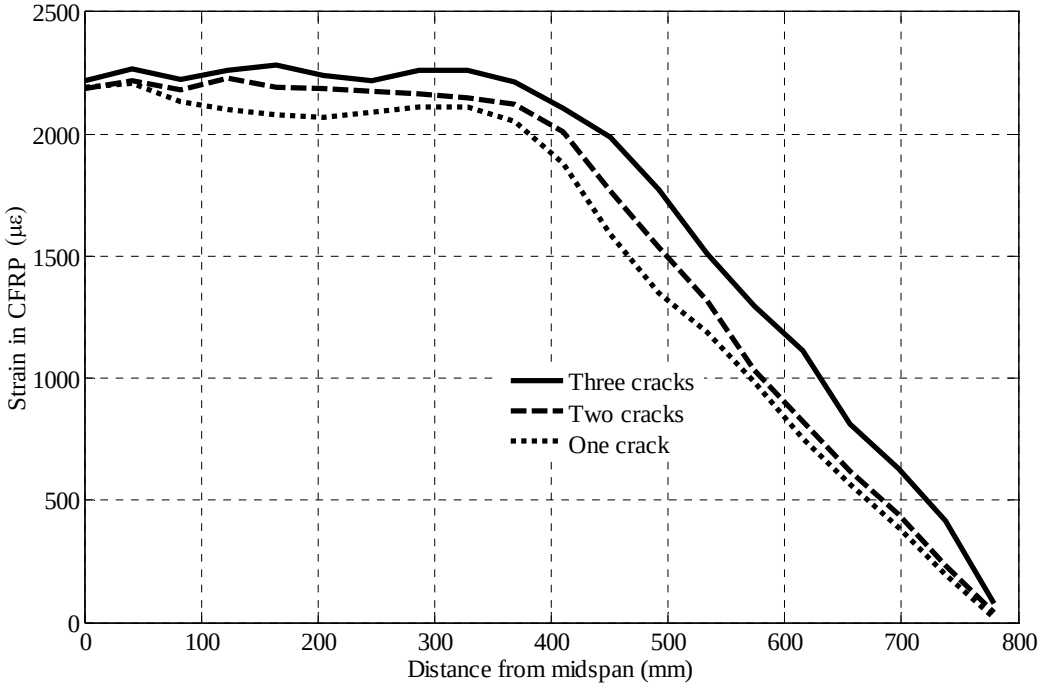

Figure (15): Axial stress in CFRP layer for beam pre-crack width cases

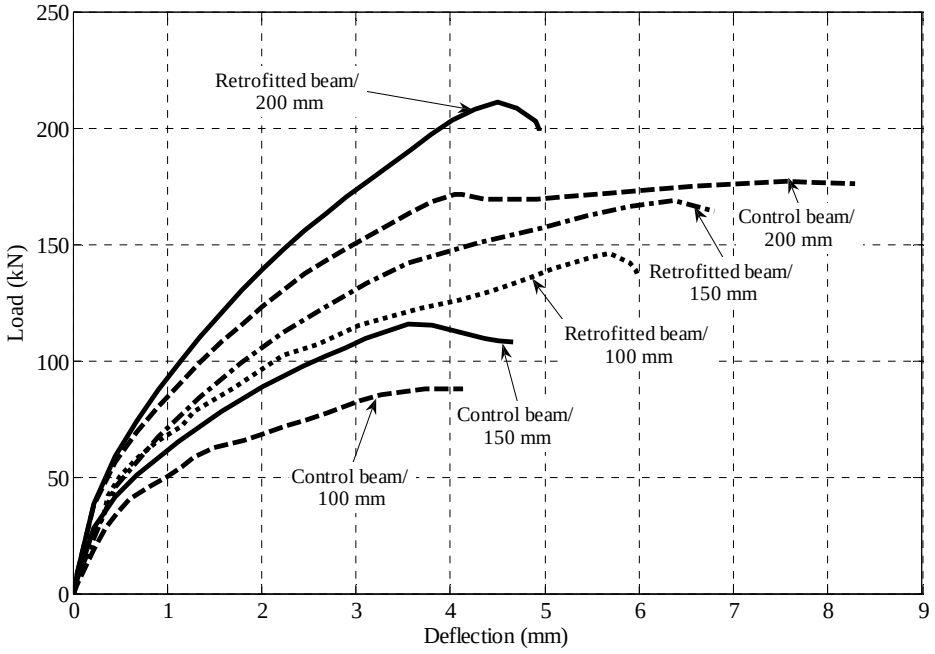

Figure (16): Load *versus* mid-span deflection for beam width models

Figure 17 shows that the beam width hardly influences the increase of load. It is noticed that the increase of load becomes higher as the beam width decreases. This is due to the fact that when the beam width decreases, the unconfined concrete area decreases compared to the case of large width of beam. This increases the interaction between the CFRP and concrete. Therefore, large concrete width reduces the degree of composite action between FRP and concrete in the first level of loading. Moreover, low rate of stress transfer forces concrete to carry a higher level of load, resulting in earlier formation and opening of flexural cracks. After cracks propagate, premature initiation of debonding occurs along the interface.

Strains in CFRP plates gradually decrease with the increase of the width of beam, see Figure 18. This is due to low stress transfer between RC and CFRP. Debonding at plate end was prevailing in all widths.

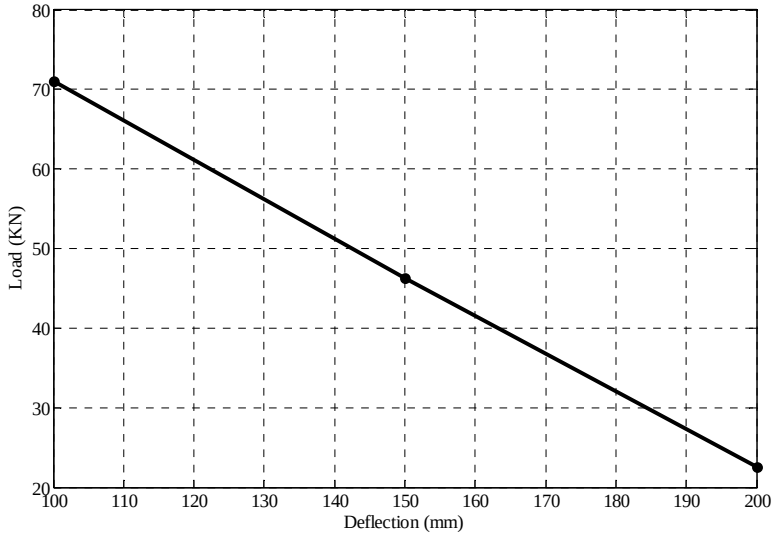

Figure (17): The percentage of increasing load capacity for beam width cases

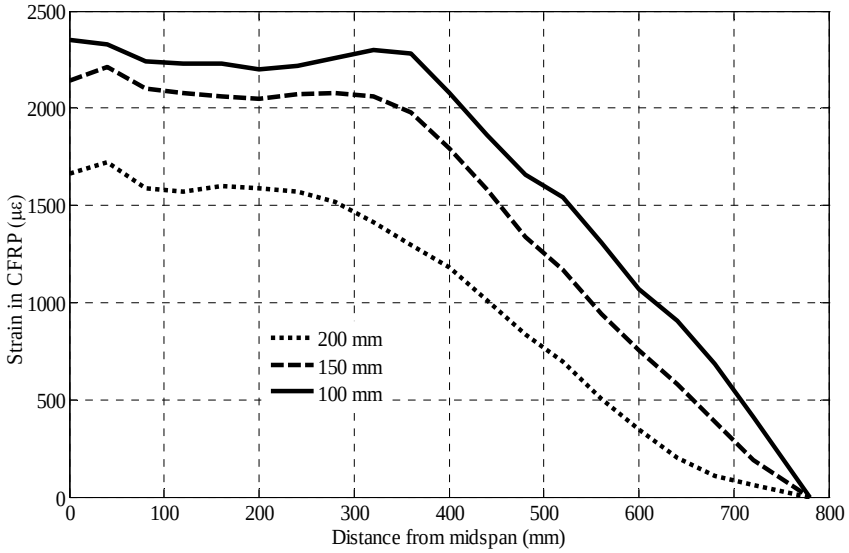

Figure (18): Axial strains in CFRP layer for beam width

CONCLUSIONS

The behaviour of reinforced concrete beams retrofitted with CFRP laminates was simulated using FEM. Mesh sensitivity was studied. Results showed that the analytical models reflected the real behaviour with accuracy. The study shows that fine mesh around the crack region at constant moment reflects better accuracy in the crack pattern.

The effects of concrete cover, internal tensile reinforcement, internal shear reinforcement, crack number and beam width on the behaviour of retrofitted beam using CFRP were studied. Conclusions derived from this study are as follows:

- Beams with high reinforcement ratio increase the percentage of load increase.
- As shear capacity increases, the potential of retrofitting increases.
- Pre-crack number affects the behaviour of the retrofitted beam.
- When the beam width increases, the opportunity to debonding becomes earlier and the potential of retrofitting utilization decreases.

REFERENCES

ACI Comitte 318. (1999). "Building code requirements for structural concrete and commentary (ACI 318-99)". American Concrete Institute, Detroit, MI.

Gorinevsky, S., Boyd, S., and Stein, G. (1993). "Optimization-based tuning of beton". C. E.-I. (1993), CEB-FIP Model Code 1990 (CEB-FIP MC90), Bulletin D'Information, No.215, Lausanne.

Hibbitt, Karlsson, Sorensen, and Inc. (2009). "ABAQUS theory manual, user manual, example manual". Version 6.9. Providence, RI.

Hillerborg, A. (1985). "The theoretical basis of a method to determine the fracture energy of concrete". Materials and Structures, RILEM 50-FMC, 108, 291-296.

Hu, H.T., and Schnobrich, W.C. (1989). "Constitutive modelling of concrete by using non-associated plasticity". J. Mater. Civil Eng. (ASCE), 1 (4), 199-216.

Obaidat,Y., Heyden, S., Dahlblom, O., Abu-Farsakh, G., and Abdel-Jawad, Y. (2011). "Retrofitting of reinforced concrete beams using composite laminates". Construction and Building Materials, 25, 591–597.

Obaidat,Y., Heyden, S., and Dahlblom, O. (2010). "The effect of CFRP and CFRP/concrete interface models when modelling retrofitted RC beams with FEM". Composite Structures, 92, 1391-1398.

Obaidat, Y., Heyden, S., and Dahlblom, O.(2013). Evaluation of parameters of bond action between FRP and concrete". Journal of Composites for Construction (ASCE), 17 (5), 626-635.

Pannirselvam, N., Raghunath, P., and Suguna, K. (2008). "Strength modeling of reinforced concrete beam with externally bonded fibre polymer reinforcement". American Journal of Engineering and Applied Sciences, 1 (3), 192-199.

Saenz, L. (1964). "Equation for the stress-strain curve of concrete". Desayi, P., and Krishnan, S. (Eds.). ACI Journal, 61, 1229-1235.

Supaviriyakit, T., Pornpongsaroj, P., and Pimanamas, A. (2004). "Finite element analysis of FRP strengthened RC beam". Songklanakarin, J.Sci.Technol., 26 (4), 497-507.

Yang, Z., Chen, J., and Proverbs, D. (2003). "Finite element modeling of concrete cover separation failure in FRP-plated RC beams". Construction and Building Materials, 17, 3-13.